Design of a Hospital Stretcher with a Semi-Active Vibration Absorption System

Patipol Thanuphol[1,*], Netirat Kaewthueng[1], Songklod Warakunphinyo[1], Sittikorn Lapapong[2], Sarawut Lerspalungsanti[2], Pinet Sriyotha[1] and Paiboon Choungthong[1]

[1] Department of Production Engineering, King Mongkut's University of Technology Thonburi, 126 Pracha-uthit Road, Bangmod, Thungkru, Bangkok, 10140 Thailand
[2]National Metal and Materials Technology Center (MTEC), 114 Thailand Science Park, Phahonyothin Rd., Klong 1, Klong Luang, Pathumthani 12120 Thailand
*Corresponding Author: patipol.thanu@gmail.com, Tel: +668-5194-2270, Fax +66-2-872-9081

Abstract

In many fields of engineering, applications of modern control have become increasingly important. One of the main benefits of modern control is an ability to design a controller to adjust and/or improve the dynamic properties of a system. This paper describes an application of modern control to design a vibration absorption system for a hospital transportation stretcher. The main objective of this work is to reduce the level of vertical vibration induced by path surface roughness as well as road disturbance by using a semi-active vibration absorption system. Modeled the stretcher with the vibration absorption system as a two-degree-of-freedom system, its equations of motion of the stretcher are derived. Measured by accelerometers mounted on the stretcher, road roughness given as the disturbance to the model is applied to investigate the performance of the designed vibration absorption system. The simulation results of the proposed system are presented and discussed.

Keywords: Hospital Stretcher, Semi-Active Vibration Absorption System, Modeling and Control of Mechanical Systems

1. Introduction

One of the current standard protocols to transport a patient is by using a hospital stretcher. Typically, a conventional hospital stretcher is composed of a steel frame and rubber wheels and is not equipped with any kinds of vibration absorption systems. Since the stretcher has no vibration absorption system, its use may cause deterioration on patients, especially those who have just gone through operations, due to the vibration induced by the unevenness of floor. To deal with this problem, there is a necessity to reduce the vibration level transferred to the patient on the stretcher. From the past, there have been many attempts to design some types of vibration absorption systems for a stretcher. Basically, there are three primary concepts of vibration absorption systems: passive system, active system, and semi-active system, and a number of control strategies have been proposed [1-4]. A passive vibration absorption system is a mechanism composed of springs and shock absorbers or dampers. This passive system has some fundamental limitations, which is the ability to merely reduce the vibration level in some ranges of the disturbance spectrum. To improve these limitations, active and semi-active systems are developed [1], [4]. An active vibration absorption system is one of the most effective ways to isolate vibrations. The active system uses an actuator to provide an external force applied to adjust the overall dynamics of the system. Nonetheless, the active system has complexity in structure design and high cost [2], [3], and also requires a relatively large energy source to operate. Because of these drawbacks inherited in the active system, a semi-active vibration absorption system is selected in this work. The semi-active system typically utilizes a conventional spring and a variable damper to regulate vibration level.

The remainder of the paper is organized as follows: Section 2 derives the model of the stretcher with the semi-active vibration absorption system. Section 3 explains a procedure to measure road roughness. The design of the semi-active vibration absorption system is discussed in Section 4. Section 5 investigates the performance of the proposed system. The last section then summarizes the key points of this paper.

2. Modeling of Hospital Stretcher with Semi-Active Vibration Absorption System

A hospital stretcher with a semi-active vibration absorption system is modeled as shown

in Fig. 1(a). The model has two degrees of freedom, consisting of a sprung mass and an unsprung mass. The sprung mass (M) is the mass that situates on the vibration absorption system, including the mass of a patient. The unsprung mass (m) consists of the mass of the lower part of the stretcher. Both masses are connected together by a spring (k) and an adjustable damper (c).

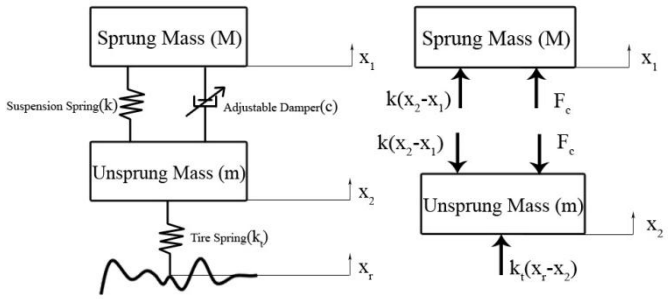

(a) (b)

Fig. 1 (a) Model of hospital stretcher with semi-active vibration absorption system, (b) Free-body diagram of the hospital stretcher model [5-6]

From the free-body diagram in Fig. 1(b) and with the help of the Newtonian mechanics, the equations of motion [6] of the model in Fig. 1(a) are as follows:

$$M\ddot{x_1} = k(x_2 - x_1) + F_c \quad (1)$$

$$m\ddot{x_2} = -k(x_2 - x_1) + k_t(x_r - x_2) - F_c \quad (2)$$

where M is the sprung mass and m is the unsprung mass. k and k_t respectively are the stiffness of the spring and tire. F_c represents the damping force that is the control effort for the system. x_1, x_2, and x_r denote the displacements of the sprung mass, the unsprung mass, and the road, respectively. The block diagram that represents Eqs. (1) and (2) is illustrated in Fig. 2.

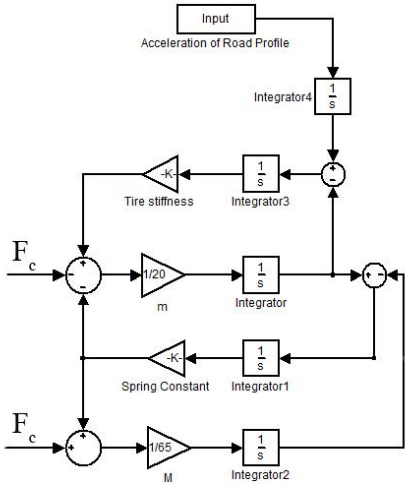

Fig. 2 Block diagram of the system

3. Road Roughness Measurement

The road roughness data are necessary in order to design the vibration absorption system and validate the fidelity of the proposed system. To measure the road roughness, two accelerometers were installed on a hospital stretcher equipped with a data-acquisition system. One obtained the acceleration of the lower part of the stretcher that would later be used as one of the spring stiffness design criteria and also given as a disturbance for the model derived in Section 2. The other acquired the acceleration of the upper part of the stretcher used to evaluate the performance of the designed system.

In the road roughness collection, the total length of course was 138 meters traveling through three types of floor: terrazzo floor, cement floor and tiled floor. The road rough data were recorded at the sampling rate of 2 kHz and then filtered by a low-pass filter with the cut-off frequency of 50 Hz to eliminate noises. The road roughness measurement was taken at the traveling speed of 1 m/s, and the mass of the subject who laid on the stretcher was 65 kg.

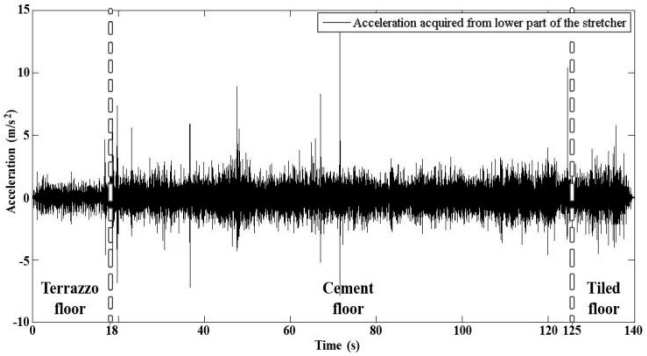

Fig. 3 Acceleration obtained from the lower part of stretcher traveling through the whole course.

Fig. 3 illustrates the acceleration acquired from the lower part of the stretcher while it was traveling through the full length of course. In the figure, the acceleration from 0-18 seconds, 18-125 seconds, and 15-140 seconds represents the roughness of the terrazzo floor, the cement floor, and the tiled floor, respectively. Further, the road roughness of these three types of floors are converted to the frequency domain via the Fast Fourier Transform (FFT) and shown in Figs. 4-6. Figs. 7-8 respectively depict the acceleration in the time and frequency domains, while the stretcher was traveling across the floor step.

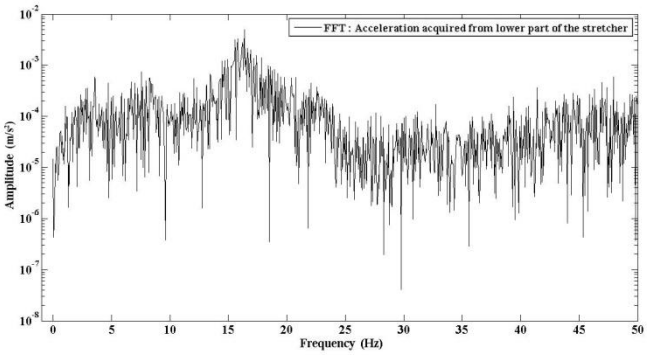

Fig. 4 Acceleration in frequency domain obtained from the lower part of stretcher traveling through terrazzo floor.

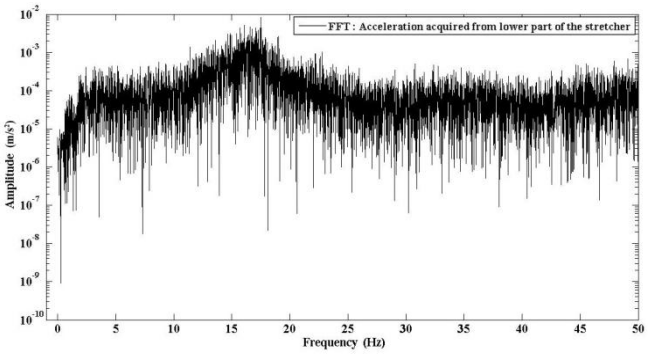

Fig. 5 Acceleration in frequency domain obtained from the lower part of stretcher traveling through cement floor.

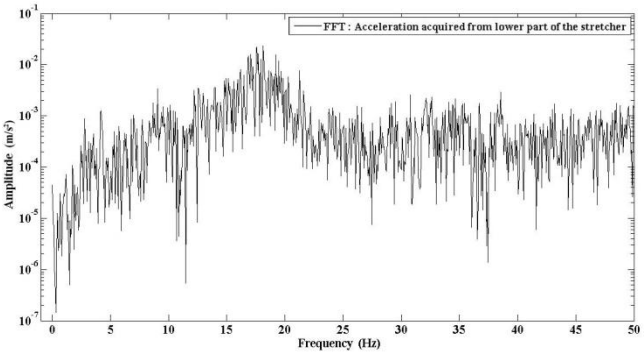

Fig. 6 Acceleration in frequency domain obtained from the lower part of stretcher traveling through tiled floor.

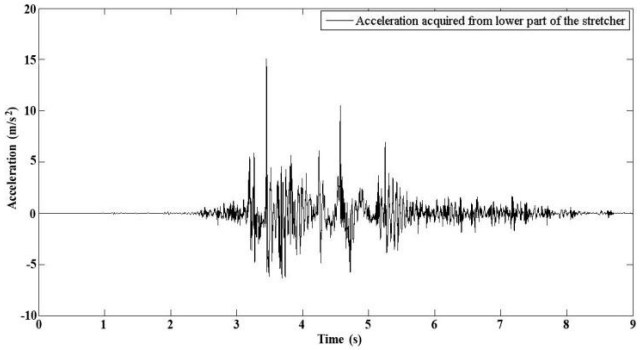

Fig.7 Acceleration obtained from the lower part of stretcher traveling across the floor step.

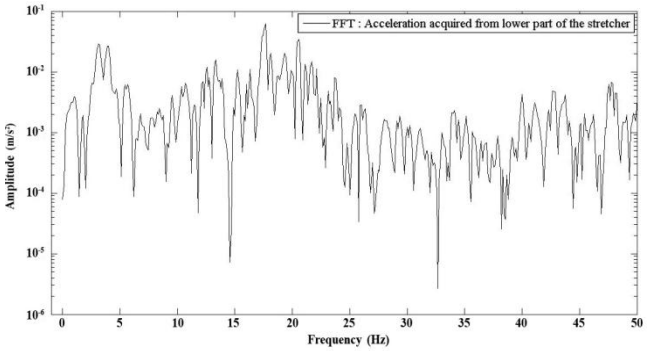

Fig.8 Acceleration in frequency domain obtained from the lower part of stretcher traveling across the floor step.

4. Control System Design

4.1 Selection of spring stiffness

This section describes a procedure of spring stiffness selection. To calculate a proper value of spring stiffness, the transmissibility ratio of the system is first derived. Substituting the term F_c in Eqs. (1) and (2) by $c(\dot{x_2} - \dot{x}_1)$, the equations of motion can be rearranged in the matrix form as:

$$\begin{bmatrix} M & 0 \\ 0 & m \end{bmatrix}\begin{bmatrix} \ddot{x}_1 \\ \ddot{x}_2 \end{bmatrix} + \begin{bmatrix} c & -c \\ -c & c \end{bmatrix}\begin{bmatrix} \dot{x}_1 \\ \dot{x}_2 \end{bmatrix} + \begin{bmatrix} k & -k \\ -k & k+k_t \end{bmatrix}\begin{bmatrix} x_1 \\ x_2 \end{bmatrix} = \begin{bmatrix} 0 \\ k_t x_r \end{bmatrix} \quad (3)$$

Considering the case in which the damping is negligible (c = 0) and applying the Laplace transform and Cramer's rule, Eq. (3) becomes

$$x_1 = \frac{k_t x_r . k}{(-m\omega^2 + k + k_t)(-M\omega^2 + k) - k^2} \quad (4)$$

Introducing the following parameters:

$\omega_{n_1} = \sqrt{\frac{k}{M}}$; natural frequency of sprung mass

$\omega_{n_2} = \sqrt{\frac{k_t}{m}}$; natural frequency of unsprung mass

$f = \frac{\omega_{n_1}}{\omega_{n_2}}$; natural frequency ratio

$u = \frac{M}{m}$; mass ratio

$r_1 = \frac{\omega}{\omega_{n_1}}$; frequency ratio of sprung mass

$r_2 = \frac{\omega}{\omega_{n_2}}$; frequency ratio of unsprung mass

Eq. (4) can be expressed as the transmissibility ratio described in Eq. (5).

$$\frac{x_1}{x_r} = \frac{1}{[1 + uf^2 - (r_1 f)^2][1 - r_1^2] - uf^2} \quad (5)$$

To examine the effect of the spring stiffness on the system, a group of spring stiffnesses is selected and the transmissibility ratios corresponding to these stiffnesses are plotted in Figs. 9-10.

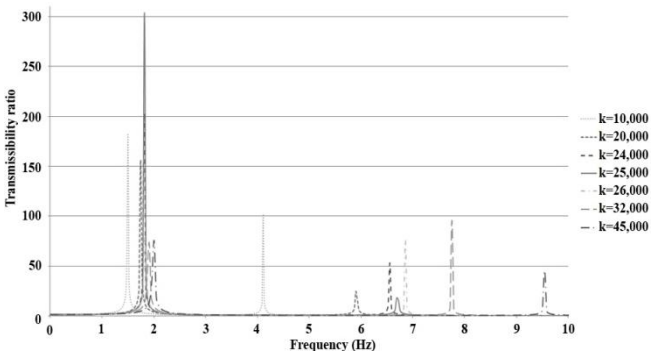

Fig. 9 Transmissibility ratio of the system with varied spring stiffnesses

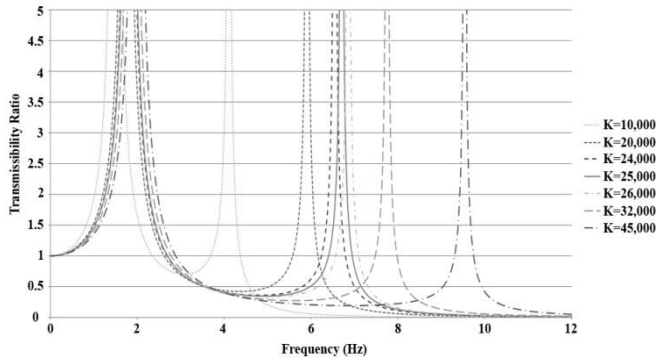

Fig. 10 Closer look of transmissibility ratio of the system with varied spring stiffnesses

From the figures, it can be noticed that the more the spring stiffnesses are, the further the distances between the two peaks are. Other than the design criterion based on the transmissibility ratio, the spring deflection is also taken into consideration. Table 1 summarizes the static spring deflection once compressed by a 60-kg load, the frequencies at the peaks in the transmissibility ratio plot, and their corresponding transmissibility ratio values. From the table, it can be seen that the spring stiffness of 25,000 N/m gives the best trade-off performance for the system. Although this value of spring stiffness returns the highest transmissibility ratio at the first peak, it gives the lowest one at the second peak. Further, from the road roughness shown in Section 3, it is obvious that the amplitudes of acceleration in the high frequency range is considerably larger than those in the low frequency range (1-2 Hz). Thus, the low value of the transmissibility ration in the high frequency range is more desirable.

4.2 Design of controller

This section discusses a design of control system used to control a damping force in an adjustable damper in the vibration absorption system equipped with the stretcher. Fig. 11 illustrates the block diagram of the control system designed to regulate the acceleration of the sprung mass ($a_{sprung\ mass}$) by adjusting the damping force (F_c). A PD controller was chosen in this work, because of its simplicity and effectiveness to deal with transient responses. By manual tuning, the values of the proportional and derivative gains of the PD controller which give optimal vibration absorption are obtained: K_p = 450, K_d = 9. These values not only give an acceptable range of the actuator force, but also return an effective result to suppress the vibration level.

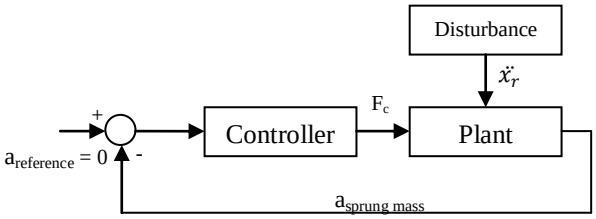

Fig. 11 The block diagram of the control system

Table1 Selection of spring stiffness

Spring stiffness (N/m)	10,000	20,000	24,000	**25,000**	26,000	32,000	45,000
Spring deflection (M=60kg)* (cm)	5.89	2.94	2.45	**2.35**	2.26	1.83	1.31
Frequency at the first peak (Hz)	1.4	1.74	1.81	**1.8**	1.82	1.91	2
Transmissibility at the first peak	181.56	156.25	203.11	**303.79**	78.20	73.43	75.61
Frequency at the second peak (Hz)	4.1	5.89	6.55	**6.69**	6.85	7.75	9.54
Transmissibility at the second peak	101.91	24.10	53.08	**17.61**	76.58	95.73	45.29

*The lowest typical mass of patent (50 kg) + sprung mass of stretcher (10 kg)

5. Results

According to the design of vibration absorption system, simulation would be tested to check how the system works for vibration absorption and observe how effective it is. The simulation can be done by giving the collected road rough data to the model derived in Section 2 as a disturbance and the feedback of the sprung mass acceleration is compared to zero then given to the controller for the proposed algorithm.

By giving these following parameters to the model, the simulation is completed. Table 2 shows the parameters used for the simulation.

Table 2 Parameters used for simulations

Parameters	Value
Sprung mass*	75 kg
Unsprung mass	20 kg
Spring stiffness	25,000 N/m
Tire spring stiffness[7-8]	15,000 N/m
Proportional gain	450
Derivative gain	9
Reference acceleration	0

*Averaged mass of patient (65kg) + sprung mass of stretcher (10 kg)

The simulation results regarding the performance of the designed vibration absorption system are illustrated in this section. As mentioned in Section 3, the vertical vibration of the stretcher are measured on three types of floor in terms of road roughness, including terrazzo floor, cement floor and tiled floor. Furthermore, the measurement was carried out on the way across. The obtained data have been filtered with the cut-off frequency of 50 Hz and given to the simulation model derived in Section 2. The simulation was carried out based on the spring stiffness of suspension and PD controller values, which are determined on a basis of criterion as described in Section 4. In this section, the simulation results are presented to compare the level of vibration, represented by vertical acceleration in time and frequency domain, of the stretcher with the designed vibration absorption system and the conventional one. Based on the results, the performance of the vibration absorption system can be determined.

As presented in Fig. 12, the acceleration obtained from the simulation on three types of floors including on the way across in time domain was reduced by means of the proposed vibration absorption system.

Fig. 13 illustrates the simulated acceleration in frequency domain which has been reduced by the vibration absorption system. Based on the determined spring stiffness, the amplitudes of the vertical acceleration are higher than ones without the vibration absorption system at a low frequency level of approximated 2 Hz. At a higher frequency level than 2 Hz, a reduction of the amplitudes is presented.

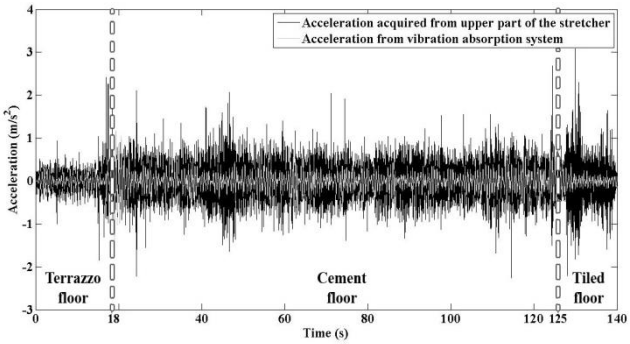

Fig. 12 The sprung mass acceleration compared to the upper part of the stretcher acceleration collected in time domain

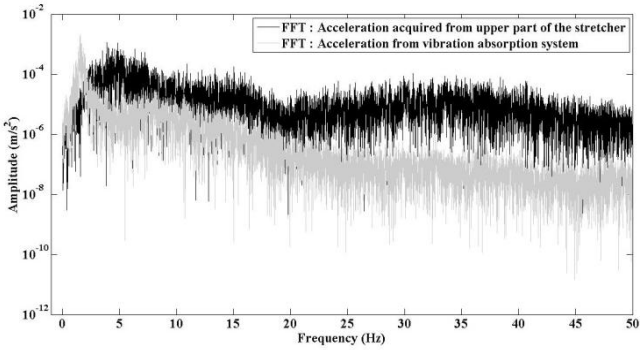

Fig. 13 The frequency domain of the sprung mass acceleration in comparison to the one measured in the upper part of the stretcher

The performance of the designed system in terms of vibration absorption on the step-floor is illustrated in Fig. 14. As it shown, the magnitudes of acceleration in m/s^2 presented in time domain are lower than the one from the measurement. This result represents the reduction of the acceleration of the sprung mass when the hospital stretcher is passing over the way across.

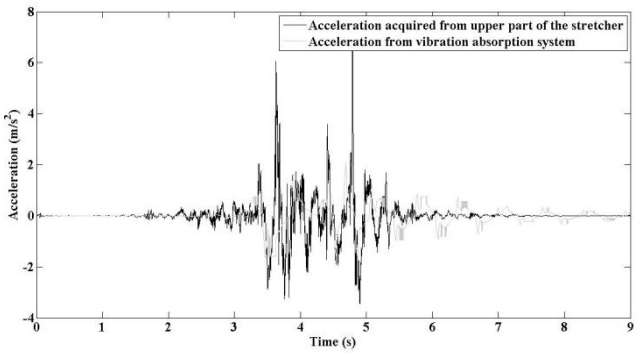

Fig. 14 The reduced sprung mass acceleration, in time domain, on the step-floor in comparison to the one measured at the upper part of the stretcher

Fig. 15 illustrates a reduction of the overall acceleration amplitude in frequency domain by means of the designed vibration absorption system.

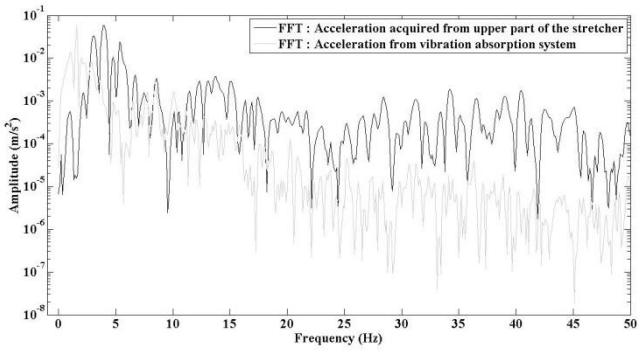

Fig. 15 The reduced sprung mass acceleration on the step-floor, in frequency domain in comparison to the one measured at the upper part of the stretcher

To compare the performance of the vibration absorption system on each type of floor, the average values of the acceleration amplitude are determined using root mean square (RMS) calculation, as presented in Table 3.

Table 3 Root mean square value of acceleration on different floor types

Types of floor	RMS value of acceleration of conventional stretcher	RMS value of acceleration of stretcher with vibration absorption system
Terrazzo floor	0.22	**0.09**
Cement floor	0.39	**0.17**
Tiled floor	0.37	**0.11**
Floor step	0.62	**0.39**

As it shown, the root mean square values of all floor types, apart from the one of the step-floor, can be decreased to about a half value of the one of the conventional stretcher by applying the vibration absorption system. In terms of the way across, the root mean square value reduction of about 60% is achieved.

6. Conclusions

The main objective of this study is to reduce the level of vertical vibration induced by path surface roughness as well as road disturbance by using a semi-active vibration absorption system. In this article, a procedure to model the vibration absorption system based on the simplified two-degree-of-freedom system described. The system parameters, such as the suspension spring stiffness is determined on a basis of the measurement of vertical acceleration of the stretcher on various types of floor. The design of controller is carried out by giving the obtained acceleration data captured by accelerometers mounted on the stretcher as a disturbance to the model.

According to the results, a reduction of the acceleration vibration level in both time and frequency domain is achieved by the application of the designed vibration absorber. The simulation results revealed that the vibration induced from road roughness decreases for about half of the value. Furthermore, a reduction of the root mean square value of about 60% was achieved.

The results obtained from this study shows a potential of the hospital transportation stretcher with the vibration absorption to reduce and/or absorb vibration induced from road. Consequently, a higher patient vibration comfort can be achieved.

7. Acknowledgement

The authors would like to express our gratitude to Pol.Lt.Col. Dr. Buncha Cheevaissarakul of the Police General Hospital for the valuable clinical information.

8. References

[1] Huseinbegovic, S. and Tanovic, O. (2009). Adjusting Stiffness of Air Spring and Damping of Oil Damper Using Fuzzy Controller for Vehicle Seat Vibration Isolation, paper presented in *Siberian Conference on Control and Communications SIBCON-2009*, Tomsk, Russia.

[2] Nguyen, L. H., Park, S., Turnip, A. And Hong, K.S. (2009). Application of LQR control theory to the design modified skyhook control gains for semi-active suspension system, paper presented in *ICROS-SICE International Joint Conference 2009*, Fukuoka, Japan.

[3] Nevala, K., M. Jaerviluoma (1997). An Active Vibration Damping System of a Driver's Seat for Off-Road Vehicles, paper presented in *4th Annual Conference on Mechatronics and Machine Vision in Practice*, Toowoomba, Australia.

[4] Ram Mohan Rao, T., Venkata Rao, G.,Sreenivasa Rao, A. and Purushottum, A. (2010). Analysis of passive and semi-active controlled suspension systems for ride comfort in an omnibus passing over a speed bump, *Research and Reviews in Applied Sciences*, vol.5(1), October 2010, pp. 7 - 17.

[5] Mo, C. and Sunwoo, M. (2002). A semiactive vibration absorber (SAVA) for automotive suspensions, *Int. J. of Vehicle Design*, vol.29, Nos. 1/2, pp. 83 – 95.
[6] Singiresu S. (2002). *Mechanical vibration*, 3rd edition, ISBN: 0-20152-686-7, Prentice Hall, Reading, Massachusetts.
[7] Wenhua Du, Dawei Zhang and Xingyu Zhao. (2009). Dynamic Modelling and Simulation of Electric Bicycle Ride Comfort, paper presented in *the 2009 IEEE International Conference on Mechatronics and Automation*, Changchun, China.
[8] Fu-Kuang Yeh, Jian-Ji Huang and Chia-Wei Huang. (2010). Adaptive-Sliding Mode Semi-Active Bicycle Suspension Fork, paper presented in *SICE Annual Conference 2010*, Taipei, Taiwan.